Plasma Mechanism for Ultraviolet Harmonic Radiation Due to Intense CO_2 Light

B. Bezzerides, R. D. Jones, and D. W. Forslund
University of California, Los Alamos National Laboratory, Los Alamos, New Mexico 87545
(Received 15 June 1981)

A theoretical explanation is presented of some observations from recent CO_2-laser experiments by introducing a novel mechanism for harmonic light emission. The theoretical model provides new insight into the properties of large-amplitude waves in the extremely inhomogeneous environment caused by strong profile modification of the critical-density plasma.

PACS numbers: 52.25.Ps, 52.35.Ht, 52.35.Mw, 52.70.Kz

Harmonic generation in laser-irradiated plasmas has been the subject of a number of experimental[1,2] and theoretical papers.[3] These studies have been confined primarily to second-harmonic (SH) emission. The analytic efforts to understand SH have relied on perturbation theory based on the assumption of a weakly nonlinear response by the plasma in which the source current for the SH is due to beats between the first-harmonic field. Higher harmonics up to the eleventh harmonic of CO_2-laser light have been reported by Burnett *et al.*[4] The relative efficiency of the emitted lines in this work was a decreasing function of harmonic number, again a result corresponding to a weakly nonlinear plasma response.

A recent paper reported the observation of CO_2 harmonic light as high as the 29th harmonic,[5] and more recently, as high as the 46th harmonic.[6] The unique feature of these data is the constant relative efficiency of the lines. It is obvious that to understand these data one must introduce a new approach which goes beyond any analysis based on mode coupling and perturbation theory. Furthermore, these data are compelling evidence for nonlinearity heretofore unexplored in the study of laser-plasma interactions. The purpose of this Letter is to understand some of the properties of this nonlinearity.

Before we discuss the nonlinear mechanism for the high-harmonic CO_2 emission, let us consider the absorption of the incident light. It is generally accepted that the dominant absorption mechanism of intense CO_2-laser light in laser-fusion applications is resonant absorption.[7] Resonant absorption in a fixed plasma density profile is a linear mechanism whereby incident light tunnels from the electromagnetic turning point and excites plasma density oscillations at the critical density, n_c, where $\omega=\omega_p$, with ω the incident light frequency and ω_p the local plasma frequency, respectively. Throughout the pulse time of the laser the plasma density is certainly not fixed and can develop a sharp plasma boundary as a result of the very substantial pressure of the intense laser light ($>10^{16}$ W/cm^2). The importance of this steepened plasma density profile will become apparent in what follows.

To understand the emitted spectrum we start with the radiation field,

$$\vec{B}(\vec{x},t)=\int\left(\frac{[\dot{\vec{j}}']}{cR}+\frac{[\vec{j}]}{R^2}\right)\times\hat{R}\,dt', \tag{1}$$

where the square brackets denote retarded time, the current $\vec{j}=-en\vec{v}$, with n and $\vec{v}$ the electron fluid density and velocity, respectively, and $\vec{R}=\vec{x}-\vec{x}'$. Introducing the Lagrangian variables $\vec{x}'=\vec{x}_0'+\vec{\delta}(\vec{x}_0',\tau')$, $\tau'=t'$, where $\vec{\delta}=\int^{\tau}d\tau'\,\vec{v}(\vec{x}_0,\tau')$ with $n_e d^3x'=n_0 d^3x_0'$, we find for the far field,

$$\vec{B}(\vec{x},t)=-\frac{e}{c^2}\left(\int d^3x_0' n_0\frac{\hat{R}\times\partial\vec{\tilde{v}}/\partial\tau}{R}(\vec{x}_0',\tau)\right), \tag{2}$$

where n_0 is the ion density, assumed fixed, and now $\vec{R}=\vec{x}-\vec{x}_0'$. We have neglected relativistic corrections, and used $\omega\delta/c\ll 1$, which requires $v_0/c\ll 1$, as we will see, where $v_0=eE_0/m\omega$ with E_0 the incident field intensity. This form for $\vec{B}$ is useful since it shows that only the fluid acceleration, albeit in Lagrangian coordinates, is needed to calculate $\vec{B}$. The justification for the use of Lagrange-transformed variables for all time, even though hot electrons are produced at high incident intensity, follows from the observation that fluid-element crossing does not occur if the full electron pressure is included in the electron Euler equation.[8] Except for the integral over the radiating material Eq. (2) is identical to the single-particle result and leads to the well-known Larmor formula for the total power radiated.

The acceleration is given by

$$\frac{\partial\vec{v}}{\partial t}+\tfrac{1}{2}\nabla v^2=-\frac{e}{m}\vec{E}-\frac{\nabla\cdot\vec{P}_e}{mn_e}, \tag{3}$$

where we have used the relation $\nabla\times\vec{v}=e\vec{B}/mc$, and $\vec{P}_e$ is the electron-pressure tensor. We now

limit our attention to a layered medium with density gradient in the x direction only. This limitation results in two important simplifications. We first note that in Eq. (3), $\partial v_x^2/\partial x \gg \partial v_y^2/\partial x$ near the critical density, since the heating is primarily in the x direction. Further, as a general result we observe that because of the symmetry of the layered problem, the functional dependence on y and t of all field quantities is in the combination $y(\sin\theta)\omega/c - \omega t$. Thus, so long as $(v_y/c)\sin\theta \ll 1$, we can write for the Lagrange-transformed acceleration from Eq. (3) ($E = E_x$, $v = v_x$)

$$\frac{\partial \tilde{v}}{\partial \tau} = -\frac{e}{m}\tilde{E}(\vec{x}_0,\tau) - \frac{(\partial P_e/\partial x)^{\sim}}{m\tilde{n}_e}. \tag{4}$$

(The tilde denotes the corresponding Lagrange-transformed quantities.) From the x component of Ampere's law and Poisson's equation the field is given by

$$\frac{\partial E}{\partial \tau} + v\frac{\partial E}{\partial x} = c\frac{\partial B}{\partial y} - v\frac{\partial E_y}{\partial y} + 4\pi e n_0 v. \tag{5}$$

Using the same arguments relied upon to derive Eq. (4) from Eq. (3), and the y component of Ampere's law, we find from Eq. (5)

$$\frac{\partial}{\partial \tau}(\tilde{E} + \sin\theta\ \tilde{B}) = 4\pi e n_0 \tilde{v}, \tag{6}$$

or

$$-(e/m)\tilde{E}(\vec{x}_0,\tau) = (e/m)\sin\theta\, B(\vec{x}_0+\vec{\delta},\tau) + \int_{x_0}^{x_0+\delta_x} dx_0'\, \omega_p^2(x_0'). \tag{7}$$

The first term in Eq. (7) is the effective driver due to the obliquely incident field, whereas the second term is the plasma restoring force. For gentle gradients Eqs. (4) and (6) lead to the usual driven-harmonic-oscillator equation of resonant absorption.

For steep density profiles numerical solutions of Eqs. (4) and (6) show that the more general form of the restoring force leads to a strongly anharmonic oscillator and almost impulselike acceleration in the critical surface region. The other terms in Eq. (4) are ignorable where the restoring force is strongly anharmonic since the pressure force is small for $\omega_{pu}^2/\omega^2 \gg 1$, with ω_{pu} the upper-shelf plasma frequency, the effect of hot-electron production on the harmonics can be ignored as it is on a timescale of $2\pi/\omega$, and finally the driving term acts only in the underdense region. Here we show by way of a model how the restoring force produces emitted harmonic light.

Consider a steeply rising density profile with plasma frequencies ω_{pu} and ω_{pl} ($\omega_{pu} \gg \omega > \omega_{pl}$), corresponding to the upper and lower density shelves, respectively (see Fig. 1). In the limit of a density jump for the profile at $x_0 = 0$, the restoring force is just $-\omega_p^2\delta$, with $\delta(x_0 = 0,\tau) = \delta$. The periodic solutions for δ and $\ddot{\delta}$ are schematically shown in Fig. 2. The solution in the overdense region is

$$\delta = (\delta)_u \cos(\omega_{pu}\theta/\omega), \tag{8}$$

whereas in the underdense region it is

$$\delta = K\sin(\omega_{pl}\theta/\omega + \varphi) + (v_0/\omega)\cos(\theta + \psi), \tag{9}$$

where $\theta = \omega\tau$, $v_0 = eE_0/m\omega$ with E_0 the effective driven intensity, and K, φ, and ψ are to be determined by the appropriate boundary conditions at the jump, viz.,

$$\delta(\bar{\theta}) = 0, \quad \delta(2\pi - \bar{\theta}) = 0, \quad \dot{\delta}(\bar{\theta}) = -\dot{\delta}(2\pi - \bar{\theta}), \tag{10}$$

with $\bar{\theta} = \omega\bar{\tau}$ and $\bar{\tau}$ the time at which δ crosses the step. With $\omega_{pu}/\omega \gg 1$, and Eqs. (8), (9), and (10),

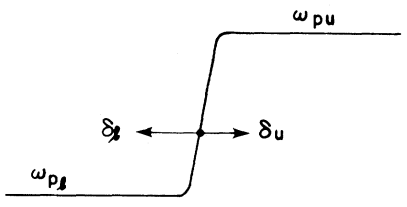

FIG. 1. Schematic representation of steep plasma density profile, showing plasma frequency corresponding to lower and upper density shelf, respectively.

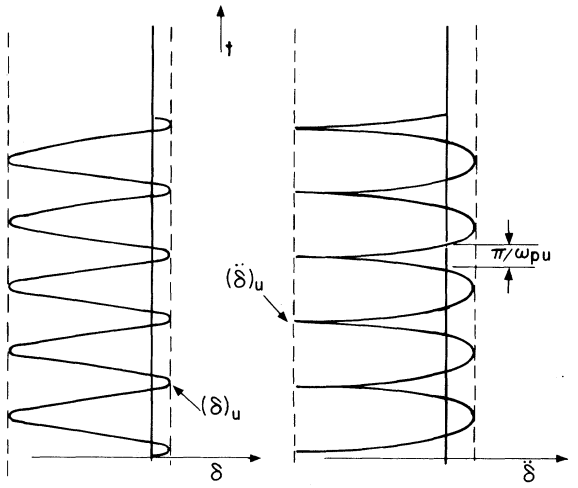

FIG. 2. Schematic representation of the displacement δ and acceleration $\ddot{\delta}$ of fluid element as it oscillates in and out of the density jump.

we find

$$K\sin\varphi = -v_0/\omega, \quad K\cos\varphi = -(v_0/\omega)\tan(\pi\omega_{pl}/\omega),$$
$$\sin\psi = 0, \tag{11}$$

and therefore,

$$(\delta)_u = \left(\frac{n_c}{n_u}\right)^{1/2} \frac{v_0}{\omega} \left(\frac{n_l}{n_c}\right)^{1/2} \tan\left[\pi\left(\frac{n_l}{n_c}\right)^{1/2}\right], \tag{12a}$$

$$(\ddot{\delta})_u = \left(\frac{n_u}{n_c}\right)^{1/2} \omega v_0 \left(\frac{n_l}{n_c}\right)^{1/2} \tan\left[\pi\left(\frac{n_l}{n_c}\right)^{1/2}\right]. \tag{12b}$$

The strong acceleration shown in Eq. (12b), which occurs essentially over the time π/ω_{pu} as seen from Eq. (8), will cause high-harmonic emission from the step region.

To estimate the emission rate into the nth spectral line $\omega_n = n\omega$, we Fourier analyze $\ddot{\delta}^2$ to obtain

$$(\ddot{\delta}^2)_{\omega_n} = \left(\frac{n_l}{n_c}\right) \tan^2\left[\pi\left(\frac{n_l}{n_c}\right)^{1/2}\right] \omega_{pu}\omega v_0^2 A\left(\frac{n\omega}{\omega_{pu}}\right), \tag{13}$$

where $A(x) \simeq 1$, $x \ll 1$, and $A(x) \to 0$, $x \gg 1$, consistent with the reciprocal relation between time and frequency for Fourier transforms. The detailed form of A is not crucial to our discussions. Now recalling that Eq. (2) leads to the well-known Larmor formula for total power emitted for a single particle, we can obtain a lower bound for the emission in the nth harmonic by assuming incoherent emission, and find

$$I_n \simeq \tfrac{2}{3}\frac{e^2}{c^3}\left(\frac{n_l}{n_c}\right)\tan^2\left[\pi\left(\frac{n_l}{n_c}\right)^{1/2}\right]\omega_{pu} v_0^2 \times \int dx_0 n_0(x), \quad \frac{n\omega}{\omega_{pu}} < 1, \tag{14}$$

$$I_n \to 0, \quad \frac{n\omega}{\omega_{pu}} \gg 1,$$

where the integral in Eq. (14) is over the depth of the radiating plasma. This result confirms the principal experimental observation of a flat spectrum for high harmonics with a well-defined cutoff, and predicts a rolloff for the spectrum at

$$n_{max}^2 = n_u/n_c. \tag{15}$$

Thus, as suggested by a recent simulation study of high-harmonic emission,[5] one can directly measure the upper density from Eq. (15) given the cutoff harmonic number. In Ref. 5, Eq. (12) was empirically determined by performing a series of numerical simulations. Here we see that it is a natural consequence of the anharmonic response of the plasma restoring force. A lower bound on conversion efficiency is obtained by using Eq. (14), with the assumption of a radiating depth equal to the skin depth of the upper density c/ω_{pu}, and by using $n_l/n_c \sim 0.1$, as indicated by high-power simulation studies. Then $\eta_n = I_n/I_{inc} \sim \frac{1}{4}\times 10^{-8} n_{max}^2/\lambda$, where λ is the vacuum wavelength in micrometers, a result which is approximately an order of magnitude smaller than the observations.[6] However, it must be remembered that the assumption of incoherent emission results in a lower-bound estimate.

To summarize the results of this paper, we have demonstrated that the principal source of high-harmonic emission is the strong nonlinear restoring force which exists when resonant absorption occurs in a highly steepened density profile, and that Eq. (12) is a general and direct consequence of such a nonlinear form of resonance absorption, and can be used with some measure of confidence to determine the density of the upper shelf. Further, the analysis conclusively shows that the source of the harmonic emission originates in the critical surface. Thus if harmonic emission is temporally and spatially resolved, one can directly measure the position and velocity of the critical surface front. Such a possibility could have wide-ranging implications for CO_2-laser–plasma diagnostics. These results are independent of the approximations used in the theoretical analysis. The finite gradient of the density profile will alter the time profile of the acceleration, but this should merely affect the rolloff of the spectrum, not the number of excited harmonics. An accurate determination of the excursion length, δ, into the low-density region of the profile would require proper account of the dissipation of the electrostatic wave in the step region of the profile, including hot-electron production, but this would only influence the calculation of the emission intensity.

The mechanism described in this paper may have application which goes beyond plasma diagnostics. It has been suggested that it may be feasible to produce vacuum-ultraviolet to soft-x-ray coherent light beams by irradiating metallic surfaces with very intense laser light.[9] We hope the simple model presented here will provide a basis for exploring this possibility.

The authors are grateful to R. L. Carman, D. F. DuBois, S. J. Gitomer, and K. Lee for useful discussions. This work was performed under the auspices of the U. S. Department of Energy.

[1]K. Eidman and R. Sigel, Phys. Rev. Lett. 34, 799

(1975).
[2]E. A. McLean, J. A. Stamper, B. H. Ripin, H. R. Griem, J. McMahon, and S. E. Bodner, Appl. Phys. Lett. 31, 825 (1977), and references therein.
[3]G. Auer, K. Sauer, and K. Baumgärtel, Phys. Rev. Lett. 42, 1744 (1979), and references therein.
[4]N. H. Burnett, H. A. Baldes, M. C. Richardson, and G. D. Enright, Appl. Phys. Lett. 31, 172 (1977), and references therein.
[5]R. L. Carman, D. W. Forslund, and J. M. Kindel, Phys. Rev. Lett. 46, 29 (1981).
[6]R. L. Carman, C. K. Rhodes, and R. F. Benjamin, Phys. Rev. A 24, 2649 (1981).
[7]V. L. Ginzburg, *The Propagation of Electromagnetic Waves in Plasmas* (Pergamon, New York, 1964).
[8]B. Bezzerides and S. J. Gitomer, Phys. Rev. Lett. 46, 593 (1981).
[9]R. L. Carman and C. H. Aldrich, in Proceedings of the Topical Meeting on Laser Techniques for Extreme Ultraviolet Spectroscopy, Boulder, Colorado, February 1982 (The Optical Society of America, to be published), and private communication.

Observation of Mode-Converted Ion Bernstein Waves in the Microtor Tokamak

P. Lee, R. J. Taylor, W. A. Peebles, H. Park, C. X. Yu, Y. Xu,
N. C. Luhmann, Jr., and S. X. Jin
University of California, Los Angeles, California 90024

(Received 18 September 1982)

Mode-conversion processes play an important role in the radio-frequency heating of tokamak plasmas. This paper reports the first direct observation of externally driven ion Bernstein waves in a tokamak plasma. The waves are only observed in mixed-species plasmas near the ion-ion hybrid resonance layer and are interpreted as being the result of linear mode conversion of the fast magnetosonic wave.

PACS numbers: 52.35.Fp, 52.50.Gj

It is generally believed that Ohmic heating alone is insufficient to produce thermonuclear ignition in tokamak plasmas and that, therefore, auxiliary heating is required. Recent experiments have demonstrated the great promise of rf heating in the ion-cyclotron range of frequencies.[1,2] However, the primary thrust of this previous work has been toward plasma heating and not wave propagation and accessibility.

The present work reports the first direct, internal, nonperturbing observation in a tokamak of externally driven waves in the ion-cyclotron range of frequencies. This has been achieved with cw far-infrared laser scattering techniques.[3] A major result has been the conclusive identification of mode conversion of the fast magnetosonic wave into an ion Bernstein wave in the vicinity of the ion-ion hybrid resonance layer. This process, predicted to occur in mixed-species plasmas,[4] is thought primarily responsible for heating results obtained in the TFR[2] and DIVA[5] tokamaks. However, until this time no direct, independent experimental verification of the existence of mode-converted Bernstein waves has been achieved.

The experiments were conducted in the University of California, Los Angeles, Microtor tokamak. The device parameters are major radius, $R_0 = 30$ cm, minor radius $= 10$ cm, $B_T = 10 - 25$ kG, $I_p = 60 - 100$ kA, $n_e = 10^{13} - 3\times10^{14}$ cm^{-3}, $T_e \leq 600$ eV, and $T_i \leq 300$ eV. Electromagnetic antennas (10 MHz $\leq \omega/2\pi \leq 35$ MHz, $P_{rf} \leq 25$ kW) were located at toroidal reference planes of 45°, 90°, 225°, and 270°. In addition, two separate far-infrared laser scattering systems were positioned at reference positions of 135° and 315°. Through simultaneous observation of scattering signals with the two lasers and by alternation of excitation antennas, toroidal propagation effects could be studied.

The far-infrared laser scattering systems both employed homodyne detection of the radiation scattered from an optically pumped cw $^{13}CH_3F$ probe laser operating at 245 GHz.[3] The output of the laser was weakly focused to a beam waist of $\simeq 2$ cm on the equatorial plane of the plasma resulting in a wave number resolution $\Delta k = \pm 1$ cm^{-1}. Variation of scattering angle allowed wave numbers k_w in the range $0 < k_w < 18$ cm^{-1} to be observed. The spatial resolution along the incident beam is dependent on the scattering angle. However, in Microtor the majority of scattering data were obtained for $\theta_s \leq 10°$ and were essential-